Developmental Biology 391 (2014) 125–132

Contents lists available at ScienceDirect

Developmental Biology

journal homepage: www.elsevier.com/locate/developmentalbiology

Resource

Resident progenitors, not exogenous migratory cells, generate the majority of visceral mesothelium in organogenesis

Nichelle I. Winters, Annabelle M. Williams, David M. Bader *

Department of Medicine, Vanderbilt University, Nashville, TN 37232, USA

ARTICLE INFO

Article history:
Received 30 October 2013
Received in revised form
1 April 2014
Accepted 3 April 2014
Available online 16 April 2014

Keywords:
Mesothelia
Organogenesis
coelomate

ABSTRACT

Historically, analyses of mesothelial differentiation have focused on the heart where a highly migratory population of progenitors originating from a localized "extrinsic" source moves to and over the developing organ. This model long stood alone as the paradigm for generation of this cell type. Here, using chick/quail chimeric grafting and subsequent identification of mesothelial cell populations, we demonstrate that a different mechanism for the generation of mesothelia exists in vertebrate organogenesis. In this newly discovered model, mesothelial progenitors are intrinsic to organs of the developing digestive and respiratory systems. Additionally, we demonstrate that the early heart stands alone in its ability to recruit an entirely exogenous mesothelial cell layer during development. Thus, the newly identified "organ intrinsic" model of mesotheliogenesis appears to predominate while the long-studied cardiac model of mesothelial development may be the outlier.

Introduction

Mesothelium is the simple squamous epithelium that lines the body wall and organs of the coelomic (pleural, pericardial, and abdominal) cavities in vertebrates. During organogenesis, mesothelial cells throughout the organism generate the visceral vasculature, provide stromal cell populations through epithelial to mesenchymal transition (EMT) (Que et al., 2008; Asahina et al., 2011; Wilm et al., 2005; Dettman et al., 1998), and influence the growth (Li et al., 2011) and differentiation (Yin et al., 2011) of the organs they cover. In the adult, mesothelial cells modulate many characteristics of the coelomic cavities including fluid and immune cell content (Mutsaers, 2002), angiogenesis (Mandl-Weber et al., 2002), and rates of fibrinolysis (Tietze et al., 1998). These features in turn regulate ischemic injury repair and adhesion formation, influence cancer metastasis, and promote fibrotic disorders (Aroeira et al., 2005; Yanez-Mo et al., 2003; Lengyel, 2010). Our understanding of the basic biological functions of mesothelium in the embryo and adult has incited interest in the therapeutic potential of this cell type. Applications currently under exploration include the modulation of EMT of the mesothelium to prevent fibrotic disorders (Loureiro et al., 2011) as well as the induction of mesothelial proliferation and migration to repair injured coelomic surfaces (Djafarzadeh et al., 2012) or even replacement of damaged cells within the organs themselves (Kovacic et al., 2012). However, the fundamental mechanisms at work in mesothelial differentiation are still largely unknown.

For decades, cardiac mesothelium (epicardium) was the only mesothelial population extensively studied during development. This intense research focus stemmed from the identification of the proepicardium—an isolated cell population that originated near the liver and sinus venosus (Ho and Shimada, 1978). This structure migrates to the heart giving rise to the epicardium, coronary vasculature, and stroma (Dettman et al., 1998). Cardiogenic splanchnic mesoderm itself does not have the capacity to generate mesothelium (Gittenberger-de Groot et al., 2000). Identification of the origin of the epicardium opened the floodgates for research and now we understand many of the cellular and molecular mechanisms leading to epicardial and coronary differentiation and are now beginning to understand important epicardial functions in the diseased or injured heart (von Gise and Pu, 2012).

We recently set out to identify the origin of mesothelium to an additional coelomic organ—the intestine. We expected mesothelial formation to proceed in the intestine as it did in the heart. To our surprise, we instead determined that unlike the heart, the avian intestinal splanchnic mesoderm housed broadly distributed mesothelial progenitors that differentiated in situ rather than from an external migratory population. This provided the first experimental evidence of an alternative model of mesothelial formation (Winters et al. 2012).

A fundamental question arises, "Is the cardiac or intestinal model the predominant mechanism at work in the generation of

* Correspondence to: 348 PRB, 2220 Pierce Ave, Nashville, TN 37232-6300, USA. Fax: +1 615 936 3527.
E-mail address: david.bader@vanderbilt.edu (D.M. Bader).

http://dx.doi.org/10.1016/j.ydbio.2014.04.003
0012-1606/

mesothelia in coelomic organs?" Here, using chick-quail chimeras, we determined the origin of pleural and pancreatic mesothelial cells. Interestingly, while the lungs and pancreas, both gut tube derivatives, form in close proximity to the proepicardium, we found that pleural and pancreatic mesothelia were both derived almost entirely from cells resident to the lung and pancreatic primordia. Conversely, we found that cardiogenic tissue is the only mesoderm capable of recruiting exogenous mesothelia during organogenesis. Thus, the current data suggest that the new "organ intrinsic" model of generating mesothelia prevails in organogenesis of the respiratory and alimentary tracts while recruitment of exogenous progenitors observed in the heart appears to be the outlier in this critical developmental process.

Results

Chick-quail chimeras have been critical as a lineage tracing technique in embryology. In using this methodology, the tissue of interest is isolated from a quail embryo and transplanted into a host chicken embryo. The transplanted material may contribute to the host embryo while the host may in turn contribute to the graft. Graft and host cells are identified by quail- (QCPN) and chick- (8F3) specific antibodies. For generation of our chimeras, transgenic donor quail embryos expressing a nuclear eYFP protein in endothelial cells (Tie1:H2B-eYFP) were utilized (Sato et al., 2010). This allows the vasculature to be visualized in whole mount and facilitates identification of graft-derived structures. As previously noted in Winters et al. (2012) and seen below, remarkable organ morphogenesis occurs in these chimeras. To determine whether the cardiac (extrinsic origin) or intestinal (intrinsic origin) model of mesotheliogenesis is observed variant organogenic models, we generated heart, lung and pancreas chick-quail chimeras and examined the mesothelium of these chimeric organs.

Ectopically transplanted hearts recruit an "exogenous" mesothelium

Quail heart tubes were isolated prior to attachment of the PE (Hamburger and Hamilton stage 12–14) and were completely devoid of mesothelial progenitors. These grafts were transplanted into the developing right abdominal cavity of a host chick embryo to determine whether cardiogenic mesoderm could generate mesothelium from endo- or exogenous sources. This protocol results in the juxtaposition of grafted material with parietal peritoneum and its resident mesothelium.

At seven days post-transplantation (7DPT), cardiac grafts were tube-like in shape (Fig. 1A, arrow) with a vascular attachment to the host (Fig. 1B, arrowhead). It is important to note that all surviving grafts analyzed here, whether they be cardiac, pleural, or pancreatic in nature, had a mesenteric connection to the body wall establishing vascular continuity with the host cardiovascular system undergoing remarkable morphogenic differentiation (Figs. 1–4 and S1, 3, and 4). Mesothelium of the mesenteric connection was continuous with mesothelium of the parietal peritoneum. These hearts also underwent spontaneous, rhythmic contraction. Immunohistochemical analyses revealed the vast majority of QCPN-positive cells within the transplant were cardiomyocytes visualized by striated patterns of staining with antibodies to both myosin and actin (Fig. 1C–H). Quail endothelial/endocardial cells were also identified within the graft-derived heart (Fig. 1H, arrows). Interestingly, chick cells (QCPN-negative) made up the mesothelium/epicardium of these hearts (Fig. 1I–L, arrowheads) and were arranged in a cytokeratin-positive epithelial layer (arrowheads) facing the coelom. The underlying submesothelial layer (Fig. 1J–L, asterisks) was also chick host-derived. The host origin of the mesothelial epicardium was further confirmed by staining for the chick cell marker 8F3 which co-localized with cytokeratin (Fig. 1M–P, arrows).

We next incubated host embryos to 14DPT to determine whether the observed mesothelial configuration was transient or retained throughout development. At 14DPT, the graft-derived hearts exhibited spontaneous contractions and were connected to the host via mesentery-like attachments (Fig. S1A–B). Remodeling of the myocardium and endocardium was even more pronounced with myocardium surrounding a blood-filled lumen (Fig. S1C–D) with extensive trabeculation (Fig. S1E–F, arrows). It should be noted that quail graft-derived hearts while undergoing significant morphogenetic transition are smaller than age-matched host hearts. The difference in size of the host and graft hearts is likely due to the intrinsic difference in size of the two organisms and it is also possible that the grafting protocol impedes growth. Importantly, the epicardial mesothelium of grafted hearts (arrowheads) and an underlying sub-mesothelial layer (asterisk) were clearly host-derived (Fig. S1G–H). MF20 staining of myocytes clearly delineates the epicardial/myocardial boundary (Fig. 1 and S1). The lack of QPCN staining of epicardial cells in both mesothelial and sub-mesothelial components of the epicardium indicates that this layer is host-derived (Fig. 1). In areas lacking a sub-mesothelial layer, the chick-derived mesothelium (arrows) was directly juxtaposed to quail-derived myocardium (Fig. S1I–L). Thus, heart tubes isolated prior to PE attachment and grown ectopically were unable to generate a mesothelium endogenously but instead recruited these cells from host tissue and maintained them throughout development.

We next transplanted quail heart tubes isolated after PE attachment and initial epicardium formation (HH19–20) to determine whether these hearts retained the ability to recruit exogenous mesothelial cells. At 7DPT, the graft-derived hearts were organized with a lumen and surrounding myocardium (Fig. 2A–B). Endothelial/endocardial cells were found throughout the myocardium and lining the lumen (Fig. 2C–D, arrowheads). The mesothelium covering the surface of the graft-derived heart was QCPN-positive demonstrating it originated from the transplanted tissue (Fig. 2E–H, arrows). Importantly, while chick cells were found scattered throughout the graft-derived heart tube demonstrating the ability of host cells to invade the graft (Fig. 2I–J, arrows), none were observed within the mesothelium (arrowheads). Thus once invested with a mesothelium, the transplanted heart losses its ability to recruit this cell type.

Pleural mesothelium is derived from an intrinsic source of progenitors

We next transplanted HH13–15 quail paired lung buds into host chick embryos to determine the origin of respiratory mesothelium. Lung buds develop as endodermal outgrowths from the foregut that branch into the surrounding splanchnic mesoderm. Grafts obtained from HH13–15 stage embryos containing quail lung primordia consist of simple endoderm and splanchnic mesoderm and are completely devoid of a mesothelial covering as evidenced by the lack of a cytokeratin-positive simple squamous epithelium on the coelomic surface of the primordium (Fig. S2). The epithelial endoderm in situ (arrows, Fig. S2B) and of the graft (arrows, Fig. S2C) is cytokeratin-positive. We have previously shown that mesothelial differentiation in gut derivatives occurs later in development at HH29 at which time this simple squamous epithelium is also cytokeratin-positive (Thomason et al., 2012). Thus at day 0, transplanted tissue is remarkably simple in structure and lacks a mesothelial covering.

At 7DPT, the grafts had formed a central gut tube and two lungs. The graft-derived lungs appeared very similar to the host lungs at this time although smaller in size (Fig. 3A–B). Upon sectioning, we found an ordered array of airways and vasculature

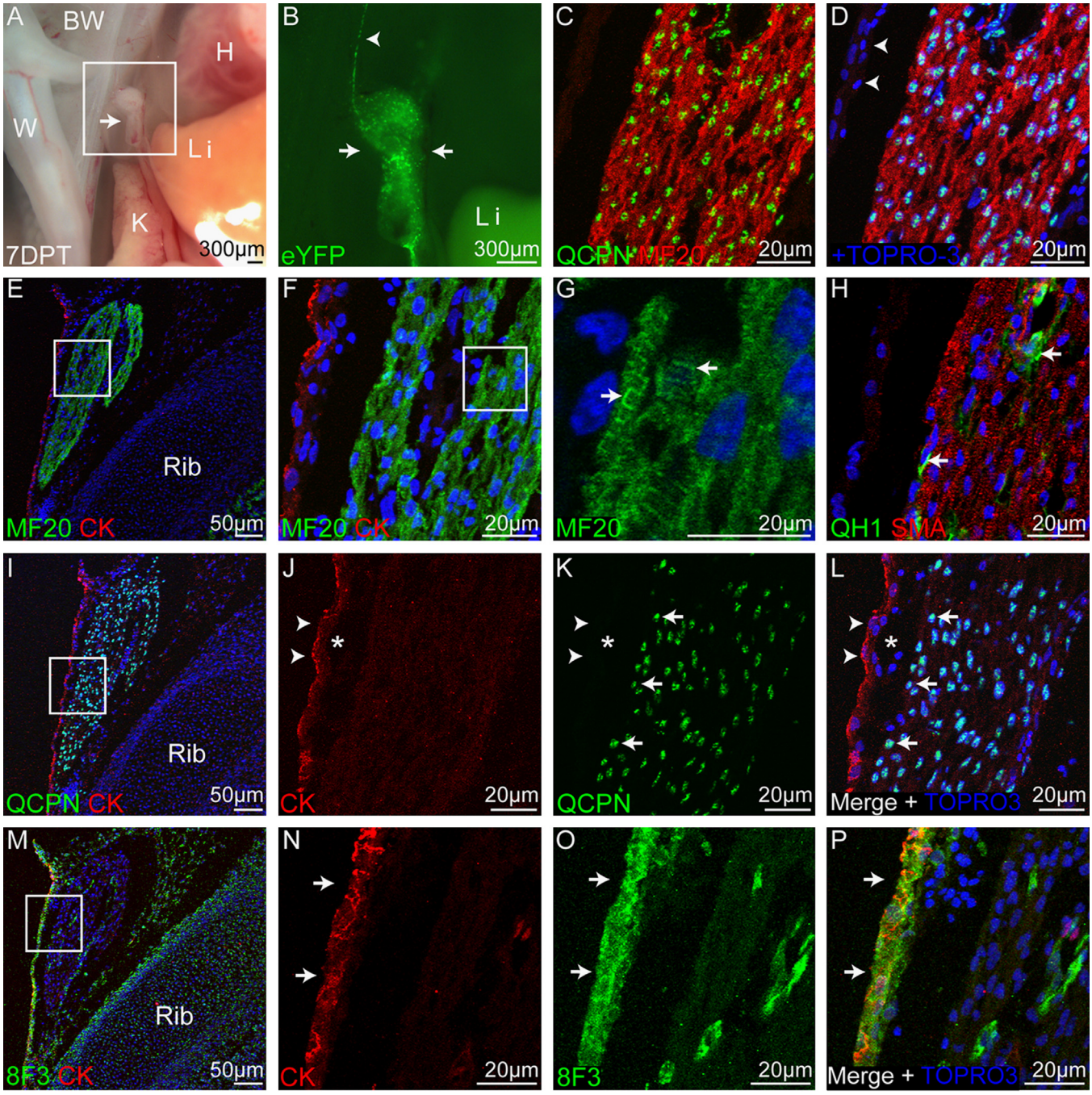

Fig. 1. Quail heart tube isolated without proepicardium 7DPT. Representative 7DPT graft-derived heart. (A) Graft developed within the coelomic cavity of the host in close proximity to the body wall (BW), liver (Li) and kidney (K) and was tube like in shape (arrow). (B) Whole mount eYFP fluorescence. A blood vessel (arrowhead) extended from the graft (arrows) to the host. (C) Quail cells (QCPN-positive) within the graft are myosin (MF20)-positive suggestive of cardiomyocyte differentiation. (D) Neighboring QCPN-negative cells are also negative for MF20 (arrowheads). (E) Low power image demonstrating myosin staining within the graft-derived heart. (F) Higher power of boxed area in (E). (G) Higher power of boxed area in (F) demonstrates striations consistent with sarcomere formation (arrows). (H) Endocardial/endothelial cells marked by the antibody QH1 were found within the graft (arrows). (I) Graft-derived heart was covered by a cytokeratin-positive surface mesothelial layer. (J–L) Higher power of boxed area in (I). The surface mesothelium was QCPN-negative (arrowheads) and had an underlying mesenchymal layer of cells (asterisks). (M) The graft-heart was surrounded on all sides by chick cells (8F3 positive). (N–P) Higher magnification of boxed area in (M). 8F3 co-localized with cytokeratin demonstrating the host origin of the graft mesothelium. BW, body wall; H, heart; K, kidney; Li, liver; W, wing.

derived from the grafted tissue (Fig. 3C) similar to wild type avian lungs. Airways were lined with a continuous mucosal cell layer (arrows) and a broken smooth muscle cell layer (arrowheads), both of quail origin (Fig. 3D). The blood vessels (arrowheads) resided in the mesenchyme of the lung encircling the airways (asterisks, Fig. 3E–F). Grafts exhibited both esophageal (Fig. 3G) and tracheal formation exemplified by cartilage differentiation with its characteristic perichondrium and developing lacunae (Fig. 3H; See Bloom and Fawcett, Twelfth edition, pages 182–183 for description of cartilage development) within the central gut tube structure. Thus, lung differentiation in the grafted tissue mirrored that on seen with differentiation in situ.

The mesothelium in grafted lungs at 7DPT was derived almost completely (95% average) from QCPN-positive cells (Fig. 3I–J, arrows). Very few chick cells were recruited into the graft at this time and those present were clearly not mesothelial in nature

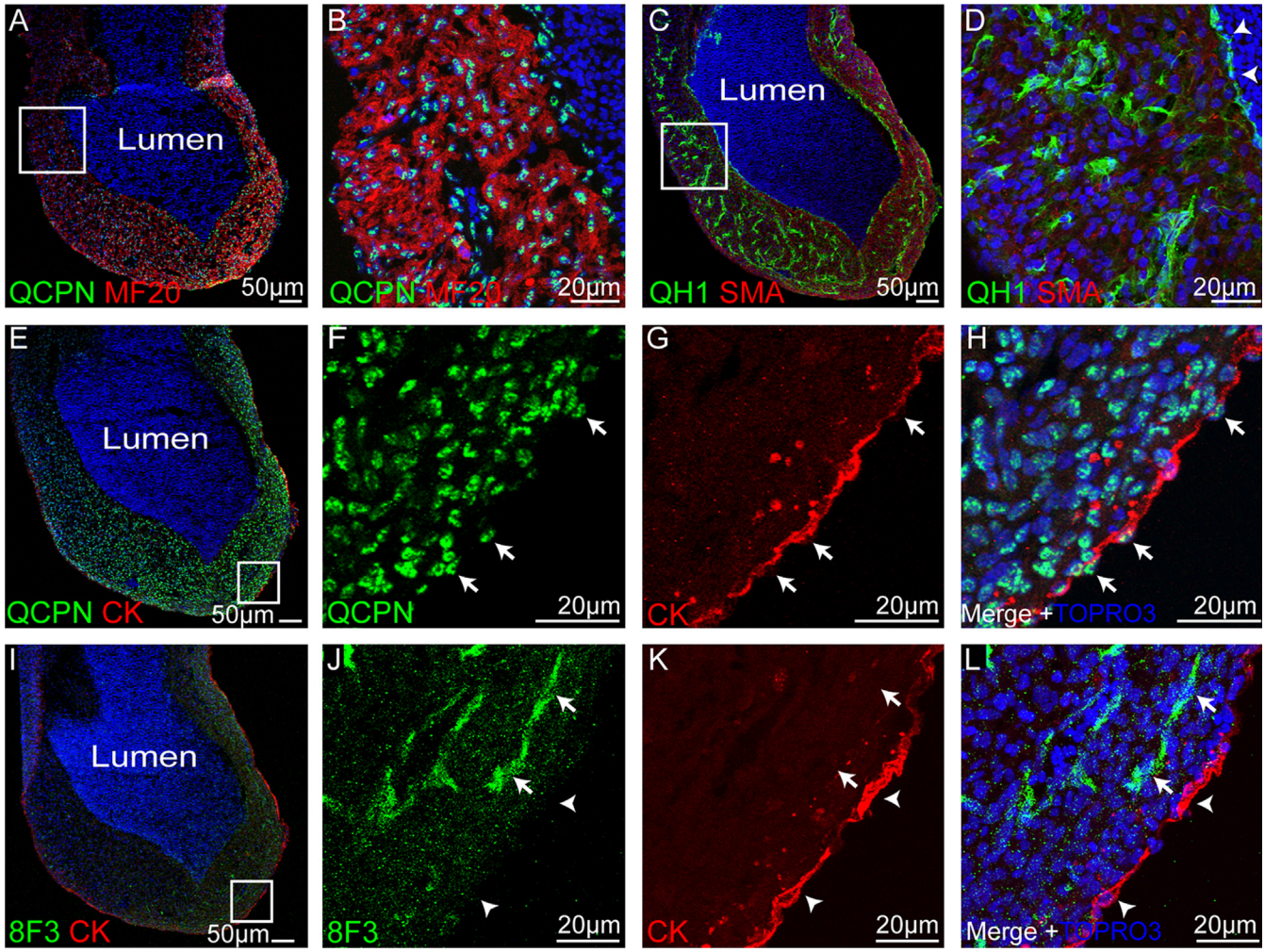

Fig. 2. Quail heart tube isolated with attached proepicardium/epicardium 7DPT. Heart tubes were isolated from HH19–20 quail embryos after the PE had attached and the epicardium had partially formed. (A) QCPN-positive myocytes encircled a blood filled lumen. (B) Higher magnification of boxed area in (A). (C) Quail endothelial/endocardial cells (QH1-positive) were distributed throughout the graft-derived heart. (D) Higher magnification of boxed area in (C). Endocardial cells lined the lumen (arrowheads). (E) Low power view demonstrating cytokeratin-positive mesothelium lining the surface of the graft. (F–H) Higher magnification of boxed area in (E). The surface mesothelial cells were QCPN-positive (arrows). (I) Low power view demonstrating scattered chick (8F3-positive) cells within the graft-derived heart tube. (J–L) Higher magnification of boxed area in (I). Chick cells were found within the graft (arrows) but not within the mesothelium (arrowhead).

(Fig. 3K–L, arrows). By 14DPT, grafted lungs had acquired a dark pink color (Fig. S3A) due to the intense vascularity (Fig. S3B). The airways continued to be invested in a broken smooth muscle layer (Fig. S3C, arrowhead) and vascular smooth muscle of quail origin had differentiated around the major blood vessels (Fig. S3C–D, arrows). The mesothelium over the 14DPT lung was on average 84% QCPN-positive (Fig. S3E–G, arrows) and 8F3 staining revealed only rare positive host-derived cells within the mesothelium (Fig. S3H–J, double arrow). It should be noted that the mesothelium of control quail lung differentiated in situ at day 14 was on average 83% QCPN-positive suggesting that QCPN does not mark 100% of quail cells and/or that the perinuclear antigen is more difficult to detect in mesothelial cells flattened with differentiation or embryonic age. Taken together, these data demonstrate that the vast majority of avian lung mesothelium is generated and maintained from a population of progenitors intrinsic to the splanchnic mesoderm of the developing lung.

Pancreatic mesothelium also arises from progenitors located within the organ primordium

We next transplanted HH13–15 dorsal pancreatic buds into the coelomic cavity of host chick embryos. We specifically chose to investigate the origin of pancreatic mesothelium as a glandular derivative of the digestive system. At 7DPT, the grafts had formed an intestinal loop (D) in which the pancreas (arrowheads) was nestled similarly to the wild type configuration of duodenum and pancreas (Fig. S4A–B). The mesothelium of the 7DPT pancreas was on average 98% QCPN-positive (Fig. S4C–D, arrows). To determine whether host mesothelium transiently covered transplanted tissue, 4DPT grafts were examined for the presence of 8F3-positive surface cells. Interestingly, chicken-derived cells were never identified on the surface of transplanted pancreas (Fig. S5) or lung tissue and examination of these grafts revealed the presence of cytokeratin-positive quail cells at the organ surface (Fig. S5; arrows). Importantly, continuity of blood flow from the host and connection to the body wall were established in these 4DPT grafts. By 14DPT, pancreatic grafts had undergone significant growth and remained in the same duodenal-pancreatic configuration (Fig. 4A–B). At this time, there was abundant glucagon and insulin expression within the graft indicating that pancreatic differentiation proceeded (Fig. 4C–D and O–P). At 14DPT, pancreatic mesothelium was principally derived from QCPN-positive cells (88% average, Fig. 4E–H, arrows), although occasional patches of host-derived mesothelium were observed in two of the five pancreatic grafts analyzed (Fig. 4I–L, arrows). 8F3-positive cells were found in clusters subjacent to the

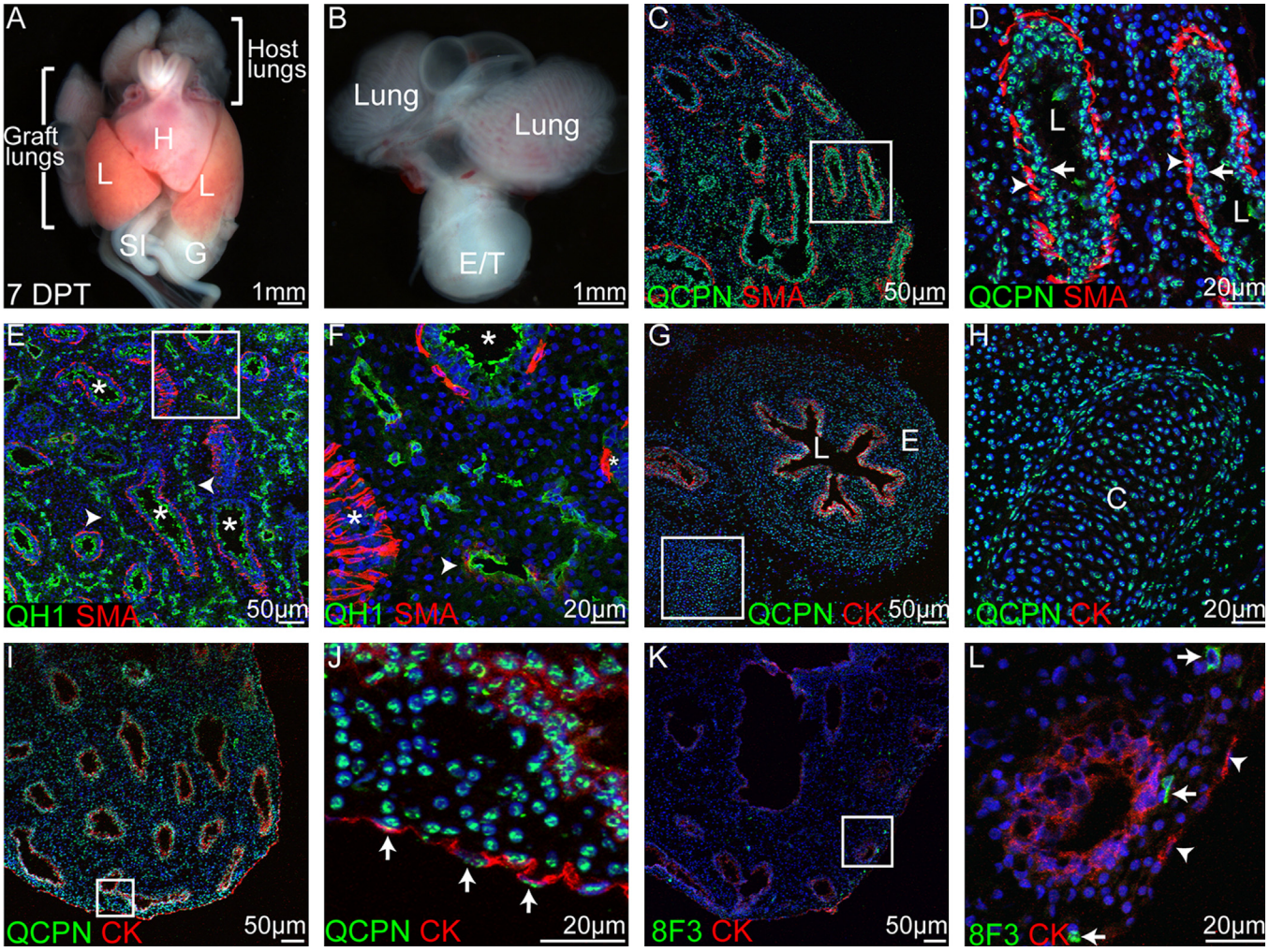

Fig. 3. Graft-derived lungs 7DPT. (A) Transplanted lung buds formed paired lungs within the coelomic cavity of the host embryo (H, heart, Li, liver, SI, small intestine, G, gizzard). (B) A central esophagus/trachea (E/T) also formed from the grafted tissue. (C) The graft-derived lungs were formed primarily of quail tissue and included a linear organization of airways. (D) Higher magnification of boxed area in (C) (L, lumen). The mucosal linings of airways were derived from quail (arrows) as was the encircling smooth muscle (arrowheads). (E) Quail endothelial cells marked by QH1 surrounded the airways (arrowheads). The mucosal epithelium was also QH1-positive (asterisks) as previously reported by Pardanaud et al. (1989). (F) Higher magnification of boxed area in (E). The major vessels exhibited limited vascular smooth muscle differentiation (arrowhead) and were localized centrally between airways (asterisks). (G) Section through the lumen (L) of the graft-derived esophagus (E). (H) Higher magnification of boxed area in (G). Near the esophageal lumen, cartilage (C) differentiation was frequently observed. (I) Low magnification demonstrating cytokeratin-positive surface epithelium. (J) Surface mesothelium was QCPN-positive. (K) Chick cells were scattered throughout the graft in low numbers. (L) Chick cells (arrows) did not contribute to the mesothelium (arrowheads). E/T, esophagus/trachea; G, gizzard; H, heart; Li, liver; SI, small intestine.

mesothelium (Fig. 4M–N, arrowheads) but the vast majority of pancreatic mesothelium, like that of the intestines and lungs, was derived from resident cells (Fig. 5).

Discussion

Mesothelia are essential cell populations that share specific functions in organogenesis and adult homeostasis. Mesothelial development has been studied for many years in the heart (Manasek, 1969). However, it is unknown whether the mechanisms of cardiac mesotheliogenesis, in particular the requirement to recruit exogenous mesothelial cell progenitors to the developing organ, are applied broadly throughout vertebrate organogenesis. We recently reported the intestine employed an alternative mechanism of mesothelial formation – generation of mesothelium from a broadly-distributed intrinsic population of progenitors (Winters et al., 2012). Still, the question remains as to whether a major conserved mechanism in this process is observed. The current study demonstrates that the lungs and pancreas of the respiratory and digestive systems respectively, also obtain the vast majority of their mesothelial lining from intrinsic progenitors. Thus, while mesothelial acquisition and differentiation in the heart is far better understood, that system appears to be the outlier being the only organ incapable of generating a mesothelium and capable of recruiting exogenous progenitors. Analysis of the small intestine, lung, and pancreas demonstrate that development of mesothelium in these settings is through the differentiation of progenitor cells intrinsic to the splanchnic mesoderm of the coelomic organ itself.

The heart has unique characteristics among coelomic organs that may offer potential explanations for this variation. All coelomic organs are derived at least in part from splanchnic mesoderm. However, the cardiac splanchnic mesoderm is specified very early in development and this early specification to a myocardial fate may prevent later mesothelial differentiation. Additionally, the lungs, liver, pancreas, and intestine include endoderm as a major component of the organ. As the cardiac splanchnic mesoderm forms a heart tube, the endoderm is excluded dorsally and thus, the heart tube would lack any positive signal originating

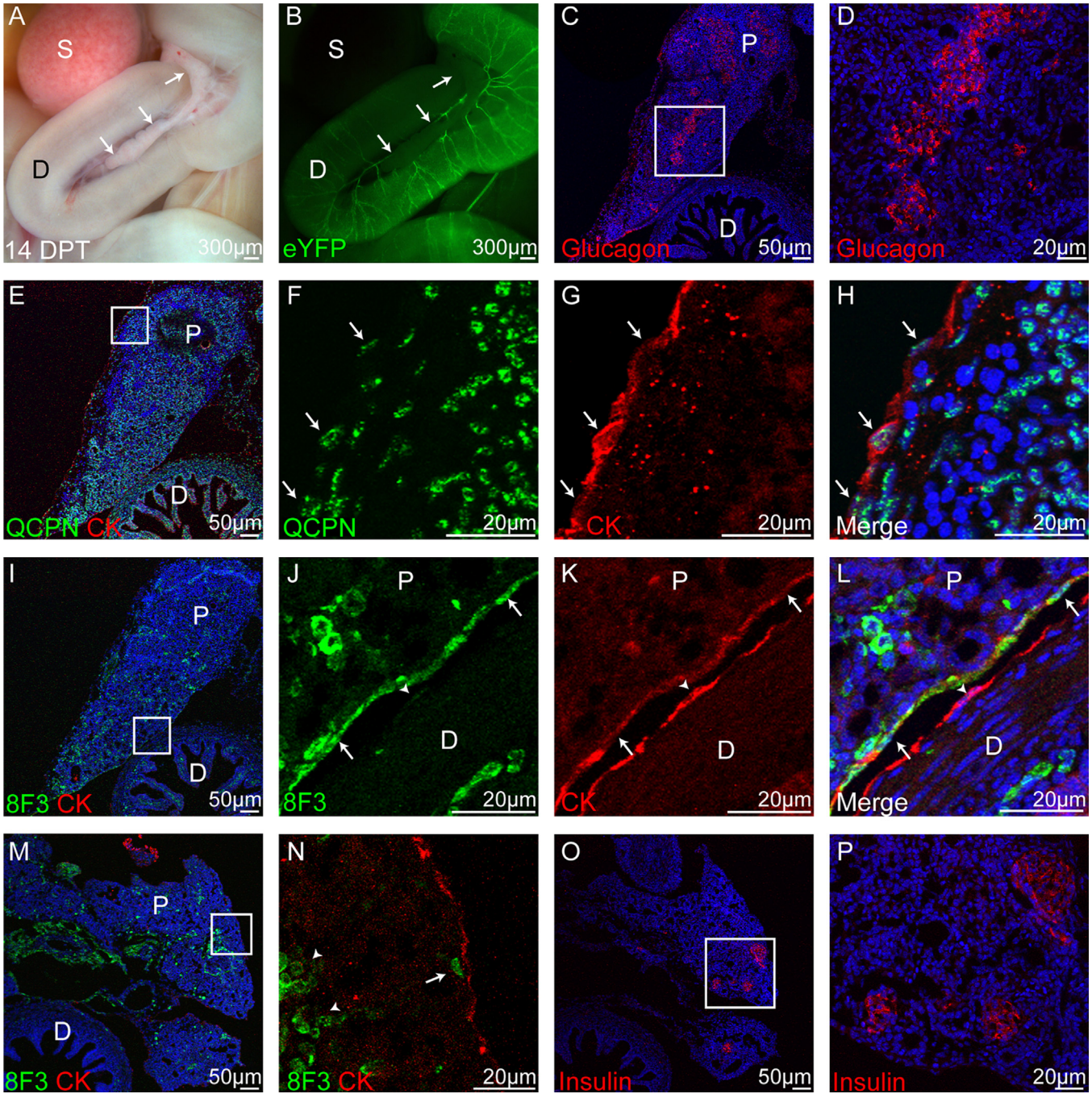

Fig. 4. Graft-derived pancreas 14DPT. (A) The grafted tissue formed a duodenum (D) and pancreas (arrows). (B) Whole mount eYFP fluorescence. (C) Within the graft-derived pancreas there were islands of glucagon positive cells (red). (D) Higher magnification of boxed area in (C). (E) Both the pancreas and duodenum were formed in large part by QCPN-positive cells. (F–H) Higher magnification of boxed area in (E). The surface cells were QCPN- and cytokeratin-positive (arrows) demonstrating their quail origin. (I) Chick cells were also distributed throughout the graft. (J–L) Higher magnification of boxed area in (I). Rare patches of surface mesothelial cells were 8F3-positive (arrows). The mesothelial cells of the nearby duodenum were 8F3-negative (arrowhead). (M) Low power view of another graft-derived pancreas and duodenum. (N) In this graft, 8F3 cells were not found within the mesothelium (arrow) and most were within clusters deep within the pancreas (arrowheads). (O–P) This graft also exhibited islet formation with insulin production (red). D, duodenum; P, pancreas; S, spleen. See also Fig. S4. (For interpretation of the references to color in this figure legend, the reader is referred to the web version of this article.)

from the endoderm required for mesothelial differentiation. Further research will be required to distinguish between these and other possibilities.

While studies on the recruitment and differentiation of mesothelia have long focused on heart development, the current study demonstrates that this model is not the principal mechanism driving development of this cell type in the intestines, lungs, and pancreas. Future studies on such organs as the gall bladder, liver and spleen will help determine whether the "organ intrinsic" model is indeed the conserved mechanism in coelomic organogenesis.

As the currently described mechanism in the generation of this cell type varies greatly from the system best understood, we must revisit the fundamental principles of mesotheliogenesis in these other coelomic organs. Currently available mouse models used for the analysis of mesothelial development in the heart may provide a rich starting point for these studies. Some of the molecular

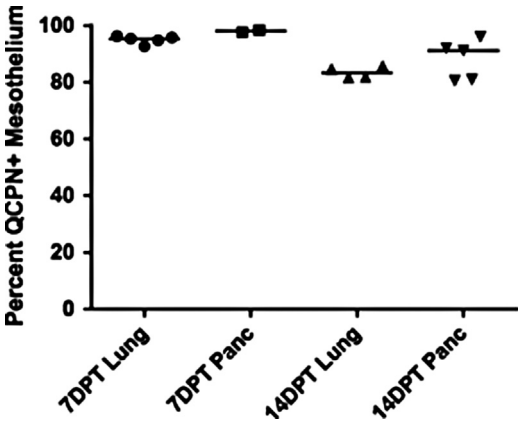

Fig. 5. Quantification of QCPN-positive mesothelium in graft-derived organs Each symbol represents a single experimental embryo. Horizontal line denotes mean value for each sample group. At 7DPT, lung and pancreatic graft mesothelia were between 93–98% QCPN-positive. At 14DPT, lung graft mesothelia were on average 84% QCPN-positive. Pancreatic graft mesothelia were on average 88% QCPN-positive at 14DPT.

mechanisms driving this process might be broadly applied throughout the embryo regardless of the origin of the progenitors. Additionally, it will be of great interest to determine whether the signaling molecules important for coronary development apply to other coelomic organs and generation of their vasculature. We would also note that the experimental paradigm employed here can be modified to probe mouse/chick chimeras where genetically modified graft tissue could be used to study the consequences of mesothelial malformation. The door is open to future research into the biology of this fascinating cell type.

Experimental procedures

Windowing

Chick (Gallus gallus) eggs incubated 2.5 days were windowed by withdrawing 4 ml of albumin and cutting a hole in the top of the egg shell. The vitelline membrane over the posterior region of HH14–17 embryos was removed with a tungsten needle. A strip of neutral red/agar was placed over the embryo to lightly stain it red. A tungsten needle was used to pierce the somatopleure anterior to the vitelline artery. All animal procedures were performed in accordance with institutional guidelines and IACUC approval.

Generation of chick-quail chimeras

Chick and quail (Coturnix japonica) embryos were staged according to Hamburger and Hamilton (1992). Lung and pancreatic buds were isolated from HH13–15 quail embryos by dissecting free the somatopleure, transecting the embryo anterior and posterior to the lung buds using the heart tube as a landmark and then cutting dorsal to the lung buds at the junction of splanchnopleure and somatopleure to free the lung buds as a single unit. The dorsal pancreatic bud was isolated by removing the PE and liver bud ventrally, transecting the embryo posterior to the pancreatic bud, and then cutting dorsally at the junction of splanchnopleure and somatopleure freeing a small section of splanchnopleure with attached pancreatic bud. This strategy was used to remove potential contamination from PE cells which develop in association with the liver bud (Ishii et al., 2007; Viragh et al., 1993). The PE, liver, and ventral pancreatic bud were dissected away before isolating the dorsal pancreatic bud for transplantation. All of these transplants are completely devoid of a mesothelial covering at this time (Fig. S2). Heart tubes were isolated from HH12–14 (without any visible PE attachment) or HH19–20 (after PE attachment and migration) quail embryos and then splayed open to expose the endocardium. Dissection was carried out in sterile Tyrode's salt solution. A single quail tissue isolate (lung buds were transplanted as a unit) was transplanted into the right lateral (future abdominal) cavity just anterior to the vitelline artery of a host chick embryo. Tyrode's salt solution with 1% penicillin/streptomycin was added to replace volume and chick eggs were sealed and incubated for 7 or 14 days.

Immunohistochemistry (IHC) and co-localization analysis

Isolated grafts were fixed in 4% formaldehyde in PBS. Cryosections were cut at 5 μm thickness. Immunohistochemical analysis of sectioned chick or quail tissue was as published in Osler and Bader (2004). The following primary antibodies were applied overnight at 4 °C: Anti-GFP (Invitrogen A11122, 1:200), Anti-smooth muscle actin (Sigma A2547 1:200), Anti-smooth muscle actin (Abcam Ab5694 1:200), Anti-sarcomeric myosin (MF20), QCPN (DSHB undiluted), 8F3 (DSHB 1:25), Anti-cytokeratin (Abcam Ab9377, 1:100), QH1 (DSHB, 1:200), Anti-insulin (Abcam Ab63820, 1:100) and Anti-glucagon (DAKO, A0565, 1:200). The following secondary antibodies were applied at a 1:500 dilution for 90 min at room temperature: Alexa fluor 488 or 568 Goat anti-rabbit (Invitrogen); Alexa fluor 488 or 568 Goat anti-mouse (Invitrogen). TOPRO-3 (Invitrogen T3605) at 1 μmol/L was applied with secondary antibody. Sections were imaged in Z-stacks using a LSM510 META Confocal with 0.4 μm optical slices. All IHC images presented in figures are Z-projections. The mesothelial layer was distinguished by morphology combined with cytokeratin staining. Nuclei within the mesothelial layer were manually identified and then subsequently identified as QCPN positive or negative.

Acknowledgments

Research was supported by NIH grant RO1 DK83234. All confocal imaging was performed through the use of the VUMC Cell Imaging Shared Resource. Core Services performed through Vanderbilt University Medical Center's Digestive Disease Research Center supported by NIH grant P30DK058404 Core Scholarship. Monoclonal antibodies were obtained from the Developmental Studies Hybridoma Bank developed under the auspices of the NICHD and maintained by The University of Iowa, Department of Biology, Iowa City, IA 52242.

Appendix A. Supplementary material

Supplementary data associated with this article can be found in the online version at http://dx.doi.org/10.1016/j.ydbio.2014.04.003.

References

Asahina, K., Zhou, B., Pu, W.T., Tsukamoto, H., 2011. Septum transversum-derived mesothelium gives rise to hepatic stellate cells and perivascular mesenchymal cells in developing mouse liver. Hepatology 53 (3), 983–995.

Aroeira, L.S., et al., 2005. Mesenchymal conversion of mesothelial cells as a mechanism responsible for high solute transport rate in peritoneal dialysis: role of vascular endothelial growth factor. Am. J. Kidney Dis. 46 (5), 938–948.

Dettman, R.W., Denetclaw Jr., W., Ordahl, C.P., Bristow, J., 1998. Common epicardial origin of coronary vascular smooth muscle, perivascular fibroblasts, and intermyocardial fibroblasts in the avian heart. Dev. Biol. 193 (2), 169–181.

Djafarzadeh, R., et al., 2012. Recombinant GPI-anchored TIMP-1 stimulates growth and migration of peritoneal mesothelial cells. PLoS One 7 (4), e33963.

Gittenberger-de Groot, A.C., Vrancken Peeters, M.P., Bergwerff, M., Mentink, M.M., Poelmann, R.E., 2000. Epicardial outgrowth inhibition leads to compensatory

mesothelial outflow tract collar and abnormal cardiac septation and coronary formation. Circ. Res. 87 (11), 969–971.
Ho, E., Shimada, Y., 1978. Formation of the epicardium studied with the scanning electron microscope. Dev. Biol. 66 (2), 579–585.
Hamburger, V., Hamilton, H.L., 1992. A series of normal stages in the development of the chick embryo. 1951. Dev Dyn 195 (4), 231–272.
Ishii, Y., Langberg, J.D., Hurtado, R., Lee, S., Mikawa, T., 2007. Induction of proepicardial marker gene expression by the liver bud. Development 134 (20), 3627–3637.
Kovacic, J.C., Mercader, N., Torres, M., Boehm, M., Fuster, V., 2012. Epithelial-to-mesenchymal and endothelial-to-mesenchymal transition: from cardiovascular development to disease. Circulation 125 (14), 1795–1808.
Li, P., et al., 2011. IGF signaling directs ventricular cardiomyocyte proliferation during embryonic heart development. Development 138 (9), 1795–1805.
Lengyel, E., 2010. Ovarian cancer development and metastasis. Am. J. Pathol. 177 (3), 1053–1064.
Loureiro, J., et al., 2011. Blocking TGF-beta1 protects the peritoneal membrane from dialysate-induced damage. J. Am. Soc. Nephrol. 22 (9), 1682–1695.
Mutsaers, S.E., 2002. Mesothelial cells: their structure, function and role in serosal repair. Respirology 7 (3), 171–191.
Mandl-Weber, S., Cohen, C.D., Haslinger, B., Kretzler, M., Sitter, T., 2002. Vascular endothelial growth factor production and regulation in human peritoneal mesothelial cells. Kidney Int. 61 (2), 570–578.
Manasek, F.J., 1969. Embryonic development of the heart. II. Formation of the epicardium. J. Embryol. Exp. Morphol. 22 (3), 333–348.
Osler, M.E., Bader, D.M., 2004. Bves expression during avian embryogenesis. Dev. Dyn.: Off. Publ. Am. Assoc. Anatomists 229 (3), 658–667.
Pardanaud, L., Yassine, F., Dieterlen-Lievre, F., 1989. Relationship between vasculogenesis, angiogenesis and haemopoiesis during avian ontogeny. Development 105 (3), 473–485.
Que, J, et al., 2008. Mesothelium contributes to vascular smooth muscle and mesenchyme during lung development. Proc. Natl. Acad. Sci. USA 105 (43), 16626–16630.
Sato, Y., et al., 2010. Dynamic analysis of vascular morphogenesis using transgenic quail embryos. PLoS One 5 (9), e12674.
Tietze, L., et al., 1998. Modulation of pro- and antifibrinolytic properties of human peritoneal mesothelial cells by transforming growth factor beta1 (TGF-beta1), tumor necrosis factor alpha (TNF-alpha) and interleukin 1beta (IL-1beta). Thromb. Haemost. 79 (2), 362–370.
Thomason, R.T., Bader, DM, WInters, NI, 2012. Comprehensive timeline of mesodermal development in the quail small intestine. Dev. Dyn. 241, 167–1694.
Viragh, S., Gittenberger-de Groot, A.C., Poelmann, R.E., Kalman, F., 1993. Early development of quail heart epicardium and associated vascular and glandular structures. Anat. Embryol. (Berl.) 188 (4), 381–393.
Wilm, B., Ipenberg, A., Hastie, N.D., Burch, J.B., Bader, D.M., 2005. The serosal mesothelium is a major source of smooth muscle cells of the gut vasculature. Development 132 (23), 5317–5328.
Winters, N.I., Thomason, R.T., Bader, D.M., 2012. Identification of a novel developmental mechanism in the generation of mesothelia. Development 139 (16), 2926–2934.
Yin, Y., Wang, F., Ornitz, D.M., 2011. Mesothelial- and epithelial-derived FGF9 have distinct functions in the regulation of lung development. Development 138 (15), 3169–3177.
Yanez-Mo, M, et al., 2003. Peritoneal dialysis and epithelial-to-mesenchymal transition of mesothelial cells. N. Engl. J. Med. 348 (5), 403–413.
von Gise, A., Pu, W.T., 2012. Endocardial and epicardial epithelial to mesenchymal transitions in heart development and disease. Circ. Res. 110 (12), 1628–1645.